Human Molecular Genetics, 2016, Vol. 25, No. 21 4703–4716

doi: 10.1093/hmg/ddw297
Advance Access Publication Date: 29 August 2016
Original Article

ORIGINAL ARTICLE

Synaptotagmin-2, and -1, linked to neurotransmission impairment and vulnerability in Spinal Muscular Atrophy

Rocío Tejero, Mario Lopez-Manzaneda, Saravanan Arumugam and Lucía Tabares*

Department of Medical Physiology and Biophysics, School of Medicine, University of Seville, Avda. Sánchez Pizjuán, 4. 41009 Seville, Spain

*To whom correspondence should be addressed at: Lucía Tabares. Department of Medical Physiology and Biophysics. School of Medicine University of Seville. Avda. Sánchez Pizjuán, 4. 41009 Seville (Spain). Tel: +34 954556574; Fax: +34 954551769; Email: ltabares@us.es

Abstract

Spinal muscular atrophy (SMA) is the most frequent genetic cause of infant mortality. The disease is characterized by progressive muscle weakness and paralysis of axial and proximal limb muscles. It is caused by homozygous loss or mutation of the *SMN1* gene, which codes for the Survival Motor Neuron (SMN) protein. In mouse models of the disease, neurotransmitter release is greatly impaired, but the molecular mechanisms of the synaptic dysfunction and the basis of the selective muscle vulnerability are unknown. In the present study, we investigated these open questions by comparing the molecular and functional properties of nerve terminals in severely and mildly affected muscles in the SMNΔ7 mouse model. We discovered that synaptotagmin-1 (Syt1) was developmentally downregulated in nerve terminals of highly affected muscles but not in low vulnerable muscles. Additionally, the expression levels of synaptotagmin-2 (Syt2), and its interacting protein, synaptic vesicle protein 2 (SV2) B, were reduced in proportion to the degree of muscle vulnerability while other synaptic proteins, such as syntaxin-1B (Stx1B) and synaptotagmin-7 (Syt7), were not affected. Consistently with the extremely low levels of both Syt-isoforms, and SV2B, in most affected neuromuscular synapses, the functional analysis of neurotransmission revealed highly reduced evoked release, altered short-term plasticity, low release probability, and inability to modulate normally the number of functional release sites. Together, we propose that the strong reduction of Syt2 and SV2B are key factors of the functional synaptic alteration and that the physiological downregulation of Syt1 plays a determinant role in muscle vulnerability in SMA.

Introduction

Spinal Muscular Atrophy (SMA) is caused by homozygous loss or mutation of the Survival Motor Neuron 1 (*SMN1*) gene (1). Normally, the majority of SMN protein results from the expression of *SMN1* whereas a second gene, *SMN2*, produces an unstable truncated form of the protein and a small amount of full-length SMN (2). Therefore, in the absence of the *SMN1* gene, the severity of the disease depends on the amount of full-length SMN resulting from the expression of *SMN2* (*SMN2* copy number varies in the population and inversely correlates with the severity of the disease). The best-characterized SMN function is its participation in the assembly of small nuclear ribonucleoproteins (snRNPs), as part of multiprotein complexes in the spliceosomes (3).

Severe SMA (type I) patients present motor impairment consisting of rapid progressive muscle weakness of axial and

Received: July 14, 2016. **Revised:** August 22, 2016. **Accepted:** August 23, 2016

proximal limb muscles, paralysis, and early death. In the SMNΔ7 mouse model of SMA, the selective motor dysfunction is also prominent at an early stage of the disease, and mice die before two weeks of age. In this model, neurotransmitter release is significantly reduced at the neuromuscular junction (NMJ) in most vulnerable muscles (4–8), but the mechanisms responsible for this reduction and the basis of this selectivity are still not known. Here, we investigated these questions by combining functional analysis with the study of the differential expression of synaptic proteins in wild-type (WT) and SMA mouse nerve terminals of muscles affected to different degrees. We found that two synaptic proteins which have a critical role in synaptic transmission, Syt2, and SV2B, were substantially diminished in neuromuscular synapses from the *Transversus abdominis anterior* (TVA) and *Obliquus internus abdominis* (OIA) muscles, two strongly affected muscles in the disease, but less reduced in two mildly affected muscles, the *Levator auris longus* (LAL) and diaphragm. In contrast, other synaptic proteins like Syt7 and Stx1B were not changed. We also found that Syt1 is developmentally downregulated in neuromuscular synapses from vulnerable muscles (TVA and OIA). Our functional analysis revealed that the reduced postsynaptic response in SMA neuromuscular synapses was due to a reduced vesicle release probability and a decrease in the number of functional release sites. We, therefore, propose that the loss/reduction of Syt2 and SV2 determines the functional motor deficit in SMA and that the physiological differential expression of Syt1 importantly contributes to muscle vulnerability. As far as we know, this is the first report of a reduction in Syt2 and SV2B proteins associated with a human disease.

Results

In the SMNΔ7 SMA mouse model, calcium-dependent synchronous neurotransmitter release is reduced by 50% while asynchronous secretion is increased by 300% in motor nerve terminals of the TVA muscle. In the LAL, a late affected muscle, the electrophysiological alterations are much milder (6). The molecular determinant(s) of this phenotype is, however, unknown. Here, we investigated whether there was an alteration in the synaptic levels of two proteins essential for synchronous release, Syt1 and Syt2 (9–11). Syt2 is the major Syt-isoform expressed in motoneurons (12,13), and Syt2 KO mice develop a similar phenotype that SMNΔ7 mice, i.e., reduced evoked neurotransmitter release, increased spontaneous release, severe motor dysfunction, and death before three weeks of age (13). In addition, we explored the expression level of other proteins that interact with Syt1 and Syt2 and play important roles in synchronous release regulation. This study was combined with electrophysiological experiments to determine the calcium-dependence of neurotransmitter release and whether the parameters responsible for the quantal content size, i.e., the release probability (p_r) and the number of active release sites (n) were changed.

Syt2 and Syt1 levels are altered in SMA nerve terminals

To explore the possible relationship between presynaptic changes of Syt2 and Syt1 and the functional impairment, we first compared the displayed fluorescent areas of both proteins in nerve terminals of WT muscles differently affected in the disease. Syt2 labelling in TVA synapses was prominent while Syt1 was either undetectable (in 68% of terminals) or occupied very small areas (Fig. 1A, left panels). In contrast, both signals were always abundant and clearly colocalized in the LAL muscle synapses (Fig. 1A, right panels). In SMA mice, however, both Syt-isoforms were expressed in both muscles. Given these differences, we performed a quantitative analysis of Syt2 expression in neuromuscular synapses of the TVA, OIA, LAL and diaphragm muscles (Fig. 1B) and found a significant graded reduction among muscles in mutant with respect to WT (by 63 ± 4% in the TVA, $P = 0.0005$; by 67 ± 4% in the OIA, $P = 0.0005$; by 44 ± 5% in the LAL, $P = 0.0005$; by 45 ± 4% in the diaphragm, $P = 0.0005$).

Figure 1C shows the expression level of both Syt-isoforms in nerve terminals from the different muscles. The data revealed that WT muscles had substantial differences in the expression of the two Syt-isoforms; for example, in the nerve terminals of the diaphragm and LAL, the sum of both signals was 1.6- and 2.5-fold larger, respectively, than that in the TVA and OIA (dashed line). Also, we found that the total Syt-signal was always less in SMA than in WT motor nerve terminals. Together, these data suggested that the physiologically reduced expression of Syt1 in the nerve terminals of some muscles could be a determinant of vulnerability.

SV2B is decreased in SMA neuromuscular synapses

As SV2 is decreased in motor terminals of the zebrafish model of SMA (14), and this protein is known to interact with synaptotagmins and to influence its expression and trafficking (15–17), we investigated whether SMA mouse motor nerve terminals exhibits an alteration in SV2. To this end, we performed a quantitative immunofluorescence image analysis of SV2A, SV2B, and SV2C, the three isoforms expressed in mammals (18–20).

At the WT TVA synapses, all the three SV2 isoforms expressed, and the fluorescent signals occupied large areas of the terminals (Fig. 2A). In SMA littermates, however, SV2B was greatly reduced. To explore the specificity of this reduction, we quantify the mean fluorescence levels of SV2B in nerve terminals of differently affected muscles (TVA, OIA, LAL, and diaphragm). We hypothesized that the fluorescent signals should be higher in the LAL and the diaphragm than in the TVA and the OIA. We found that SV2B was significantly reduced in all four muscles of mutants, although, as predicted, more in the TVA (by 83 ± 2%; $P = 0.0005$) and the OIA (by 70 ± 4%; $P = 0.0005$) than in the LAL (by 46 ± 5%; $P = 0.0005$) and the diaphragm (28 ± 5%.; $P = 0.0005$) (Fig. 2B).

We also investigated the expression level of SV2C and SV2A in the neuromuscular synapses of the TVA and the LAL muscles. Figure 2C shows that SV2C was significantly reduced in mutant terminals of the TVA (by 51 ± 4%, $P = 0.0005$), but not of the LAL (by 18 ± 4%, $P = 0.14$). Regarding SV2A, a protein that is developmentally downregulated in nerve terminals from fast muscles like the LAL (21), we found a decrease of the signal in the mutant TVA (42 ± 4%, $P = 0.0005$) but no significant change in the mutant LAL muscle. These findings suggested a probable correlation between the reduction in the expression of the different SV2 isoforms in distinct muscles and their functional impairment.

Contrary to the above findings, the average levels of other synaptic proteins, like Stx1B, the main syntaxin isoform expressed at the mouse NMJ (22), was not different in SMA (0.84 ± 0.02) and WT (0.79 ±0.03) terminals from the TVA muscle ($P = 0.232$). Nor was the expression of Syt7 different (Fig. 2D).

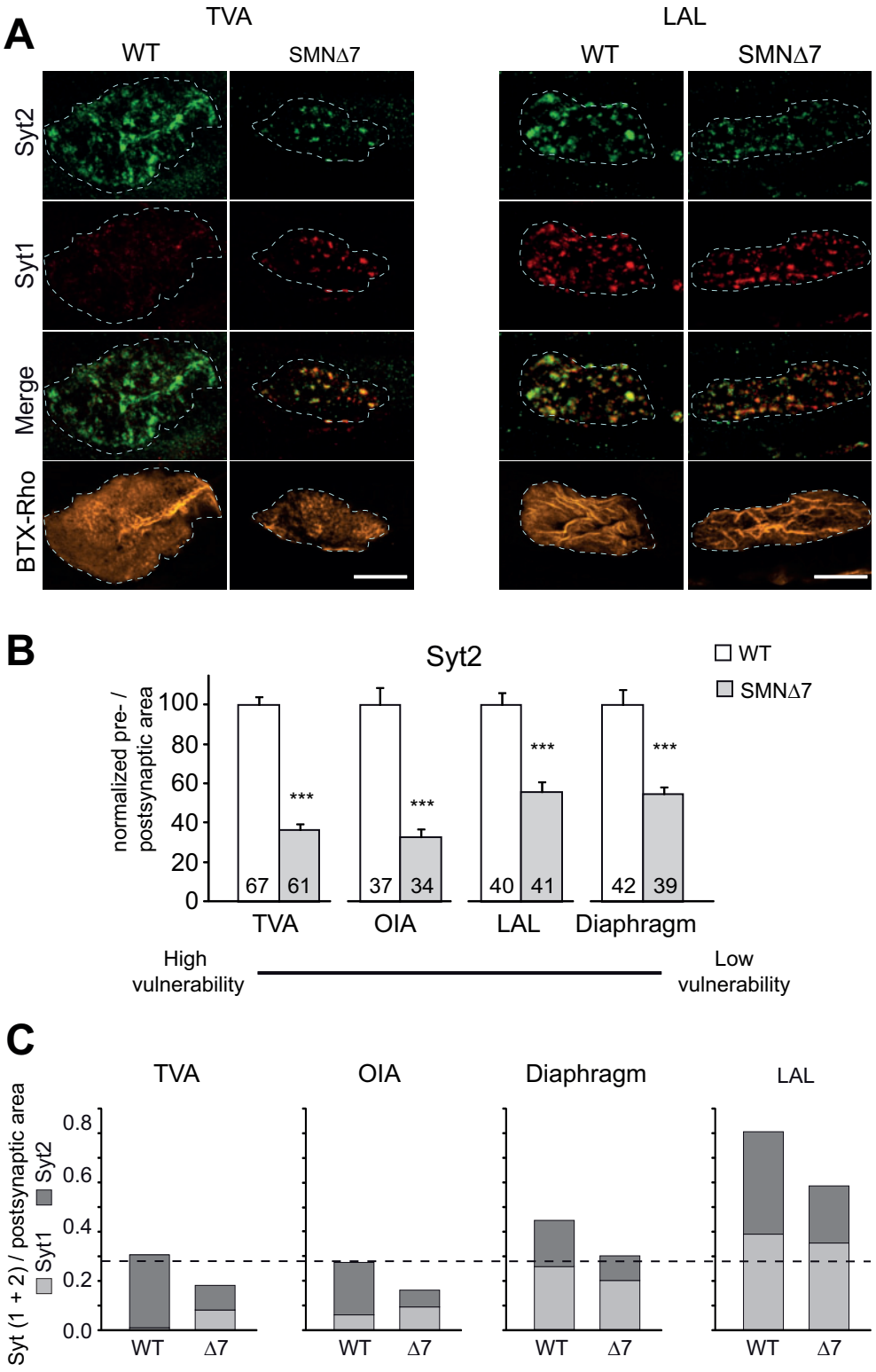

Figure 1. Differential expression of Syt2 and Syt1 in nerve terminals of severely and mildly vulnerable muscles. (**A**). Confocal Z-stack projections of representative NMJs showing the almost absence of Syt1 immunostaining (red) in WT but not in mutant motor nerve terminals of the TVA muscle (left panels). In the nerve terminals of the LAL muscle, both proteins were highly expressed (right panels). Merged images are displayed in the third panels with coincident staining in yellow. Dashed lines outline the postsynaptic surface area (lower panels). Scale bars: 10 μm. (**B**). Compared with WT, mean Syt2 signal was reduced more in the TVA and the OIA (Mann-Whitney *U* test) than in the LAL and diaphragm (Student's *t*-test) nerve terminals of mutants. Values in mutants are normalized to values of the corresponding WT littermates. Numbers of terminals measured inside bars. Data are presented as mean ± SEM. ***: $P \leq 0.0005$. (**C**). The sum of Syt1 and Syt2 signals was always smaller in mutant than in WT in all muscles. In WT synapses, the total amount of the two Syt-isoforms was much smaller in the TVA and OIA than in the LAL and diaphragm. The dashed line shows the lowest total synaptotagmin signal level found among the studied muscles in WT mice. $n = 3$-5 mice per genotype and muscle.

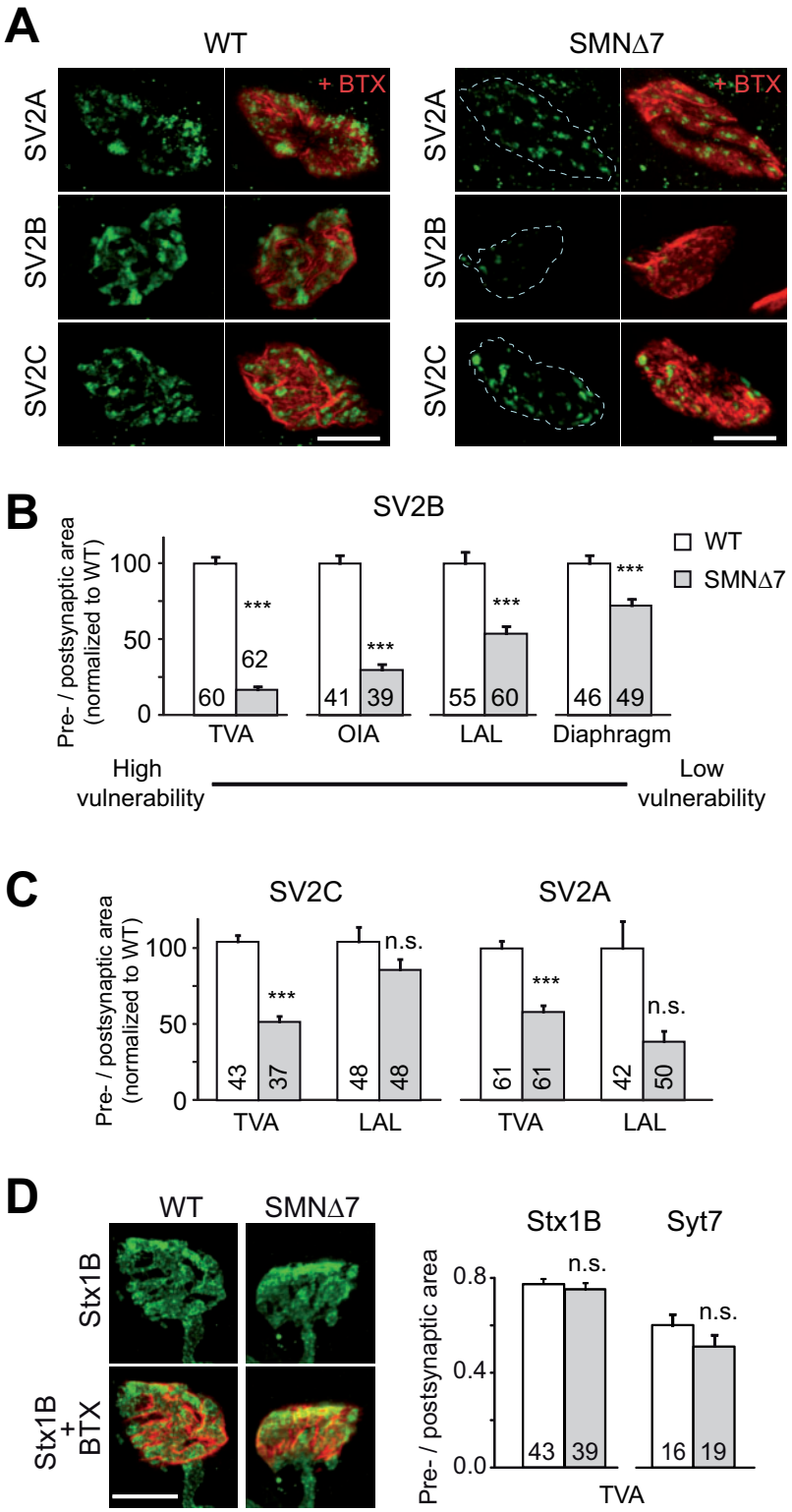

Figure 2. SV2B reduction in SMA nerve terminals correlates with muscle vulnerability. (**A**) Confocal Z-stack projections of representative NMJs of the TVA muscle showing the abundance of the different SV2 proteins isoforms labelled with their specific antibody (green), and nicotinic acetylcholine receptors labelled with BTX-Rho (red) from WT and SMNΔ7 mice. Merged images are shown in the right panels. Dashed lines outline the postsynaptic surface area. Scale bars: 10 μm. (**B & C**) SV2B mean fluorescence was greatly decreased in motor nerve terminals of the TVA and the OIA muscles, but less in the LAL and the diaphragm (B). SV2A and SV2C were also reduced in the TVA but not significantly affected at the LAL motor nerve terminals. Values in mutants are normalized to values of the corresponding WT littermates. (**D**) Confocal Z-stack projections of representative NMJs showing Stx1B labelled with a specific antibody (green), and nicotinic acetylcholine receptors labelled with BTX-Rho (red) from WT and SMNΔ7 mice (left panels). The amount of fluorescence for Stx1B and Syt7 was not different between WT and SMNΔ7 motor nerve terminals at P9-11 (middle and right graphs). Numbers of terminals measured inside bars. $n = 3 - 4$ mice per genotype and protein isoform. Error bars indicate SEM. Student's t-test in all cases except for SV2A data in the LAL, SV2B in the OIA, and Stx1B (U Mann-Whitney test). n.s.: not significant. ***: $P \leq 0.0005$.

Action potential-driven calcium influx raises release probability but does not increase the number of functional release sites in SMA terminals

The largest decrease in the total amount of the Syt-isoforms and SV2B in nerve terminals of the TVA in comparison with the LAL muscles of mutants correlates well with the degree and type of electrophysiological alterations found in these two muscles, i.e., reduction of synchronous release, anomalous increase of asynchronous release, and reduction of the readily releasable pool (RRP) size of synaptic vesicles (SVs) (6,7). Therefore, to investigate further the characteristic of the functional defect, we studied the calcium-dependence of quanta release, and the regulation of the release probability and the number of active release sites in WT and SMA mice.

Figure 3A shows that the amplitudes of the EPPs significantly increased when external calcium was raised from 1 to 3 mM in both genotypes. The relationship between extracellular calcium (0.2-3 mM) and evoked release in response to an action potential (AP) is illustrated in Figure 3B (stimulation frequency: 0.5 Hz). The fitting of the data points to a Hill function indicated that release in SMA synapses reached its maximum value at a lower calcium concentration than in WT, and the quantum content asymptotic value of the curve was about 2.5-fold larger in WT (21.1 ± 1.7 quanta) than in mutants (8.3 ± 1.3 quanta). However, neither the extracellular calcium concentration at which half-maximum release occurred (1.3 ± 0.1 mM in WT versus 1.06 ± 0.2 mM in mutants), nor the apparent calcium cooperativity, which reflects the minimum number of calcium-binding steps necessary to evoke vesicle fusion (2.9 ± 0.9 in WT and 4.1 ± 2.3 in mutants), appeared significantly different. These results show that neurotransmitter release is reduced in a broad range of extracellular calcium concentrations.

To determine whether the modest increase in the evoked neurotransmitter release (m) in SMA with extracellular calcium could be ascribed to defective rise in the average release probability (p_r), to a limited increase in the mean number of active release sites (n), or to both, we performed binomial analysis of the synaptic transmission fluctuations triggered by single APs (23–25). Interestingly, in WT p_r was constant (~0.4) with 0.75 and 3 mM extracellular calcium (Fig. 3C, dark symbols) ($P = 0.511$). This result is consistent with saturation of the release apparatus in this range (25) and predicts that the RRP size (n) increases steeply to account for the m increment. Indeed, n increased four-fold when calcium was raised from 0.75 to 3 mM ($P = 0.017$) in WT terminals (Fig. 3D, dark symbols). In mutant nerve terminals, in 1 mM calcium p_r was ~20% lower than in WT (asterisk, $P = 0.013$) but increased to the WT level at higher calcium concentrations (Fig. 3C). However, in mutants n values did not increase from 1 to 3 mM calcium ($P = 0.72$) indicating that an elevation in calcium influx through calcium channels did not increase the RRP size in SMA neuromuscular synapses, as normally occurred in WT terminals (Fig. 3D).

We then explored whether the secretion limitation persisted during repeated AP firing (20 Hz, 100 stimuli). In WT, release facilitated during the first shocks and then progressively decreased towards a plateau of similar amplitude to the initial response (Fig. 3E, upper trace, and F, black symbols). In SMA fibres, while the first EPP was much smaller than in WT (Fig. 3E, lower trace, and F, grey symbols), the next responses were characterized by a significant and sustained facilitation that made WT and mutant signals indistinguishable, suggesting that the bulk calcium accumulation during the train overcame the defect. The mean release probability during the train, calculated by binomial analysis, was 0.44 ± 0.05 in mutants, significantly larger ($P = 0.014$) than at 0.5 Hz; however, the effective RRP size (26.5 ± 8.6), was not different ($P = 0.92$) than at low frequency (25.5 ± 4). These results show that the frequency-dependent positive modulation of neurotransmitter release in mutant terminals occurred only by an increase in release probability.

Next, we raised extracellular calcium from 1 to 2 mM to explore whether release increased even further with 20 Hz stimulation. We found that cumulative release elicited by 100 shocks almost doubled (832 ± 75 quanta with 1 mM calcium versus 1562 ± 69 quanta with 2 mM calcium) in WT, while it did not change (799 ± 65 versus 779 ± 124 quanta) in SMA terminals (Fig. 3G and H). The graph of Figure 3I summarizes the effect of rising the extracellular calcium concentration and/or the stimulation frequency on neurotransmission in both genotypes. Note that at low stimulation frequency (0.5 Hz, 100 stimuli), the increase in calcium in the external solution produced 2.8-fold enhancement of total release in WT (802 ± 93 quanta at 1 mM calcium versus 2226 ± 138 quanta at 2 mM calcium), but only a 0.61-fold increase in SMA terminals (599 ± 63 in 1 mM calcium versus 975 ± 103 quanta at 2 mM calcium).

P/Q-type calcium channels mediate neurotransmitter release in SMN-deficient motor nerve terminals

The reduction in release probability at 1 mM extracellular calcium in mutants in comparison with WT neuromuscular synapses suggests that SVs experience a lower calcium concentration at release sites. The structural organization of calcium channels at the AZ (Fig. 4A) is one of the main determinants of the release probability. For example, in immature synapses (Fig. 4A, b), the distance between SVs and calcium channels seems to be larger (26), and the calcium channel type expressed is different from mature synapses (Fig. 4A, a). Additionally, a reduction in the density of voltage-dependent calcium channels (VDCCs) could also result in a low release probability (Fig. 4A, c). Then, we first investigated whether there was a change in the calcium channel type(s) that control secretion in SMA. In mouse motor nerve terminals, N-type calcium channels (Cav2.2) appear early in development and are replaced by P/Q-type calcium channels (Cav2.1) about one week postnatally (27). We used ω-agatoxin IVA (200 nM) and ω-conotoxin GVIA (1 μM) to block selectively P/Q- and N-type channels, respectively. We found that while neither of these blockers influenced spontaneous miniature endplate potential (mEPP) amplitude or frequency (data not shown), ω-agatoxin importantly reduced evoked endplate potential (EPP) amplitude in WT and SMA fibres, as illustrated in Figure 4B. The mean inhibition of release by ω-agatoxin was 98% ($P \leq 0.0005$) in WT versus 86% ($P \leq 0.0005$) in SMA terminals (Fig. 4C). Calcium-dependent release in the presence of ω-conotoxin GVIA was reduced by 63% in WT ($P = 0.03$) versus 72% in SMA terminals ($P = 0.01$). These results indicate that mainly P/Q-type, but also N-type calcium channels, participate similarly in evoked neurotransmitter release in both WT and SMN-deficient motor terminals.

To determine whether the expression level of the P/Q-type calcium channels was altered in SMA neuromuscular synapses, we compared immunostaining levels for this protein in WT and SMA nerve terminals of TVA muscles. We found that the fluorescent signal occupied larger areas in WT than in SMA terminals (Fig. 4D). Frequency distribution plots of the integrated

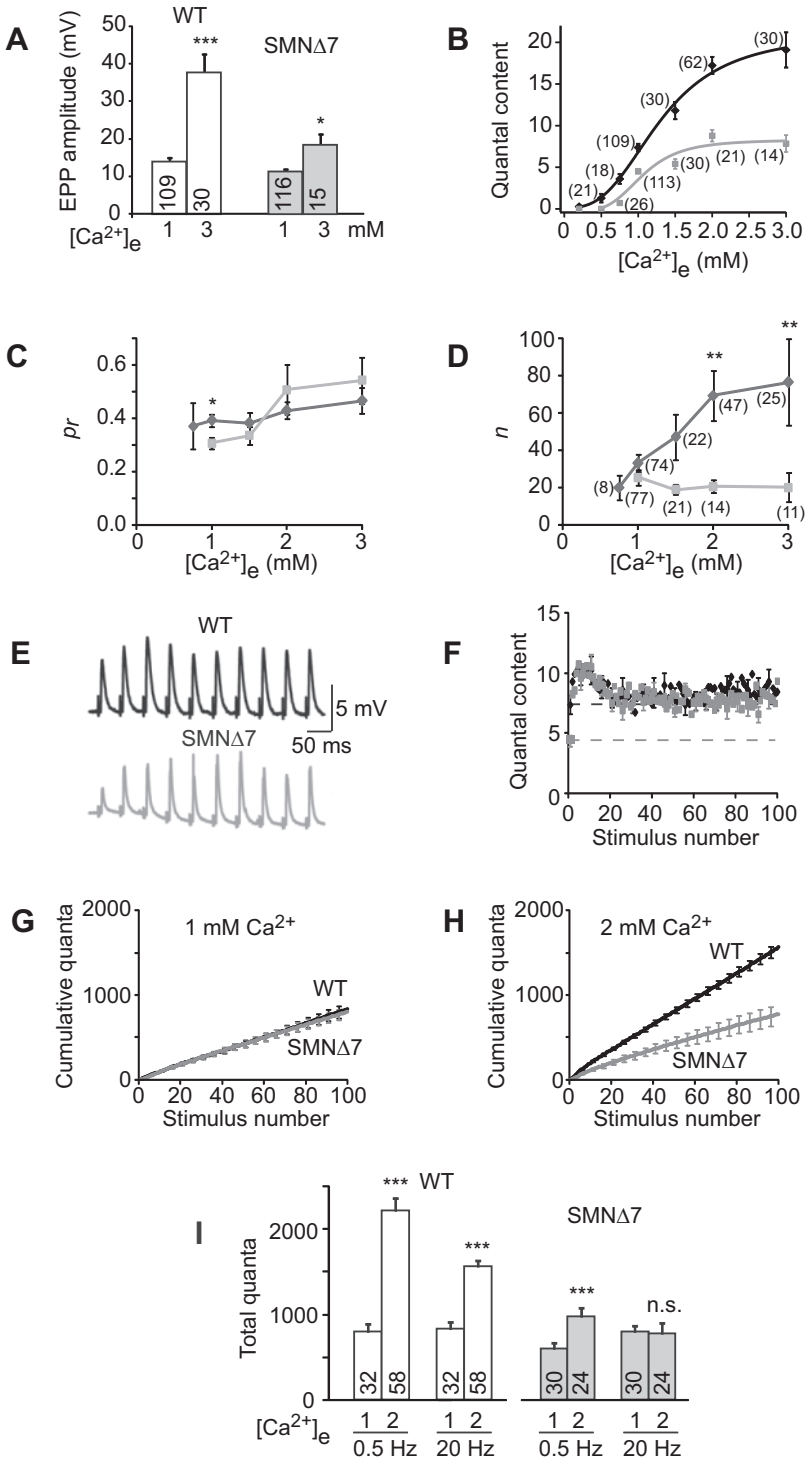

Figure 3. AP-driven calcium influx does not regulate the RRP size in SMNΔ7 motor nerve terminals. (**A**). Mean values of EPP amplitudes at 1 and 3 mM external calcium showing large synaptic responses at higher calcium concentration in both genotypes. U Mann-Whitney test. (**B**) Mean quantal content as a function of the external calcium concentration in WT (black symbols) and SMNΔ7 (grey symbols) terminals. Lines are fit of data to Hill functions. (**C & D**) Binomial analysis of quantal release at different external calcium concentrations. Release probability (p_r) did not change with calcium in WT (dark symbols, one-way ANOVA with Bonferroni posthoc analysis) but significantly increased ($P = 0.004$, Kruskal-Wallis test) in SMNΔ7 (grey symbols) terminals. At 1 mM extracellular calcium, p_r in SMA terminals was significantly less than in WT terminals (asterisk, U Mann-Whitney test) (C). The number of active release sites (n) significantly increased with calcium in WT but not in SMNΔ7 terminals (Kruskal-Wallis test) (D). (**E & F**) Representative recordings of postsynaptic potentials (EPPs) from WT and SMNΔ7 fibres with 1 mM extracellular calcium at 20 Hz stimulation. (F): mean quantal content values in WT (black) and SMNΔ7 (grey symbols) were undistinguishable except for the first responses (dashed lines). (**G & H**) At 20 Hz stimulation, SMNΔ7 terminals released the same number of quanta as WT terminals in 1 mM but not in 2 mM extracellular calcium. (**I**) In WT terminals, total quanta release by 100 shocks at 0.5 or 20 Hz increased about two-fold when extracellular calcium was raised from 1 to 2 mM (G). In SMNΔ7 fibres, elevated extracellular calcium increased release at low-frequency stimulation but not at 20 Hz. All data are presented as mean ± SEM. U Mann-Whitney test. Number of fibres recorded inside bars. $n = 3 – 15$ mice per genotype. n.s.: not significant. *: $P < 0.05$; **: <0.005; ***: $P \leq 0.0005$.

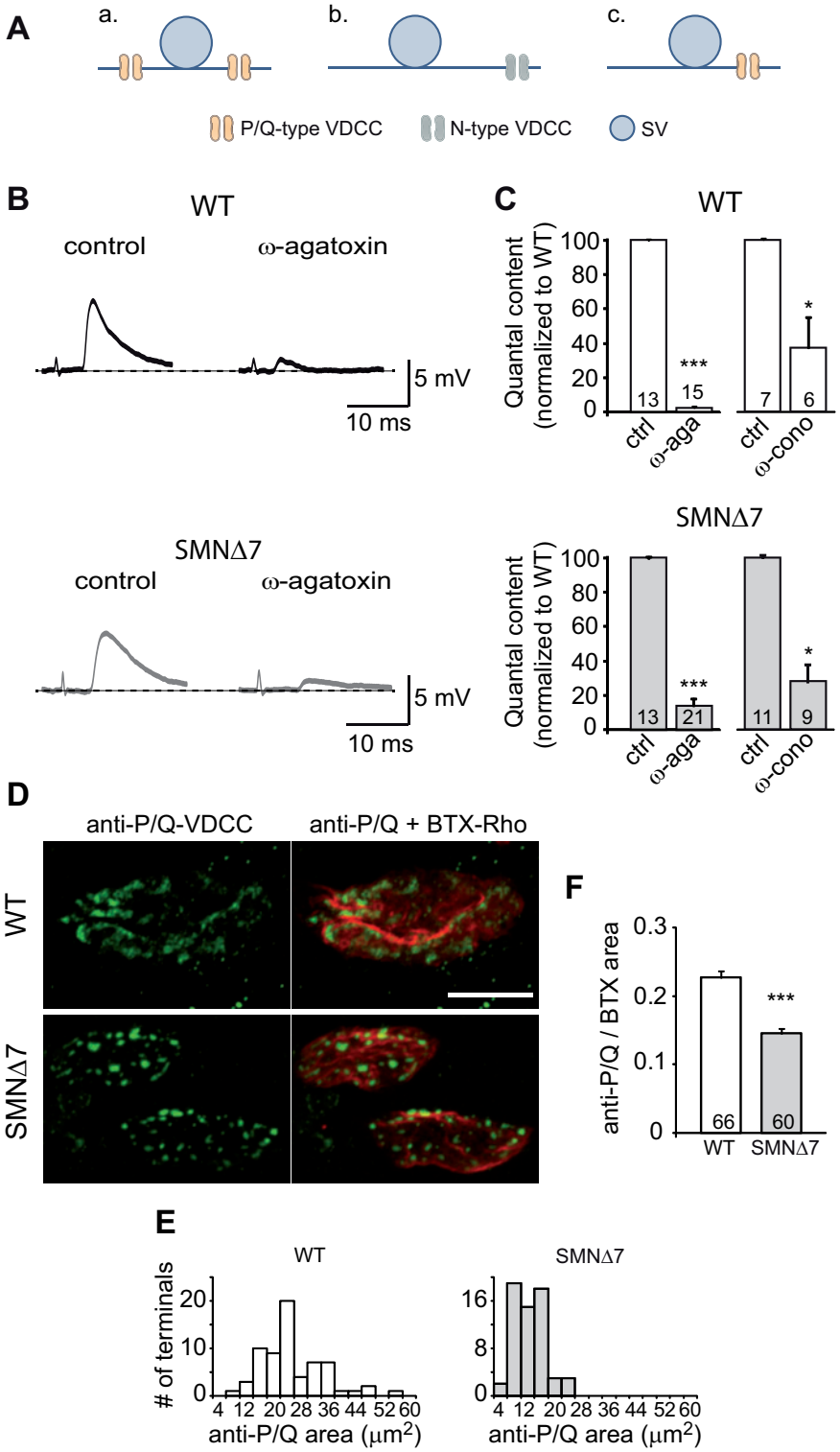

Figure 4. Reduced P/Q-type calcium channel expression in SMNΔ7 motor nerve terminals. (**A**) Schematic representation of the theoretical relationship between calcium channels and vesicles at the AZ. In mature synapses (**a**), the coupling is high and channels are P/Q-type; in immature (**b**), the distance of the calcium channels (N-type) to the release site is increased; it is also possible that a poor density of calcium channels at the AZ exists, related or not with the maturation stage (**c**). **B.** ω-agatoxin efficiently blocked P/Q-type VDCC evoked neurotransmitter release in WT and SMNΔ7 nerve fibres. **C.** Percent of quantal content reduction of evoked neurotransmitter release in WT and SMNΔ7 nerve fibres by ω-agatoxin (200 nM) and ω-conotoxin GVIA (1 μM, selective N-type VDCC blocker). (**D**) Confocal Z-stack projections of representative NMJs showing P/Q-VDCCs labelled with anti-P/Q antibodies (green) from WT and SMNΔ7 mice. Nicotinic receptors were stained with BTX-Rho (red). The P/Q fluorescence signal was more punctate in SMA than in WT terminals. Merged images are shown in the right panels. Scale bars: 10 μm. **E & F.** P/Q fluorescence was reduced in SMNΔ7 terminals. Distribution of total P/Q fluorescence area in different terminals (E). Average areas of P/Q signals normalized for end plate (BTX) area (F). Data in C & F are mean ± SEM. Numbers of terminals analysed inside bars. $n = 2$–4 mice per genotype. Student's *t*-test (C), Mann-Whitney *U* test (F). *: $P \leq 0.05$; ***: $P \leq 0.0005$.

P/Q-type channels fluorescent area per terminal showed a left-shift in SMA compared to WT (Fig. 4E), with mean values almost halved in SMN-deficient mice. When the signal area was normalized to the postsynaptic surface area (Fig. 4F), still a 36% reduction in the P/Q mean area persisted ($P \leq 0.0005$), indicating that the decrease was not due only to the smaller size of SMA NMJs. These data explain, at least in part, why nerve-evoked neurotransmitter release is decreased in SMA neuromuscular synapses.

Phorbol ester increases neurotransmitter release in SMN-deficient mice by increasing the number of functional release sites

Since the above experiments show that the number of active release sites (n) did not increase in mutants when extracellular calcium was raised (Fig. 3D), we hypothesized that the number of AZs with docked/primed vesicles was limited in these terminals. In SMA motor synapses, the number of SVs is reduced (4,6–8) what may decrease the release site occupancy (Fig. 5A, b). Alternatively or additionally, the reduced levels of Syt2 and SV2 in these terminals (Fig. 1 and 2) may alter docking and priming (28–32) (Fig. 5A, c). To explore these possibilities, we used a phorbol ester. Phorbol esters stimulate transmitter release in normal frog and mouse NMJs (25,33,34), and in CNS neurons (35,36). Phorbol esters are functional analogs of diacylglycerols (DAGs) and act by activating PKC and Munc-13 (37,38). Activated Munc-13, in turn, unfolds and activates the SNARE protein syntaxin and, thereby, promotes the formation of the SNARE complex (39). In addition, it has been also suggested that Munc-13 activation reduces the energy barrier for fusion (40,41). Therefore, we predicted that the phorbol ester would have no effect in the mutant if the main problem were the decreased number of vesicles in the terminal.

For these experiments, 5-10 fibres were first recorded in the absence of the drug (control), and a similar number 10-20 min after adding phorbol-12,13-dibutyrate (PDBu, 1 μM) to the extracellular solution. In the presence of the drug, the average EPP amplitude in response to 0.5 Hz stimuli increased both in WT (227%) and in SMA (∼300%) terminals ($P = 0.0005$). No change in the mean mEPP amplitude over control values was observed, but mEPP frequency was highly potentiated in WT (∼923%) and SMNΔ7 (∼452%) terminals (Fig. 5E and F) ($P = 0.0005$), as previously described in other synapses. Control experiments using the vehicle alone (DMSO 0.06%) had no significant effect on mEPP amplitude or frequency ($P > 0.05$). As expected by the rise in EPP amplitude and the absence of effect on mEPP amplitude, mean quantum content (Fig. 5D), and cumulated quanta after 100 stimuli were increased by PDBu, ∼189% in WT (660 ± 59 versus 1247 ± 114; $P = 0.0005$), and ∼153% in SMA terminals (522 ± 73 versus 797 ± 87 cumulated quanta; $P = 0.001$).

To investigate whether the enhancement of secretion was due to a rise in the probability of release (p_r) and/or in the number of release sites containing fusion-competent synaptic vesicles (n) we next performed binomial analysis of both parameters. Our study revealed that PDBu increased the number of active release sites, that is, the size of the effective RRP, in WT by ∼300% (control: 39.5 ± 12; PDBu: 127.5 ± 29.2; $P = 0.002$), and by ∼265%, (control: 28.8 ± 12; PDBu: 76.1 ± 33; $P = 0.009$) in SMA terminals, without having a statistically significant effect in p_r in neither case (Fig. 5G and H). This result highly contrasts with the inability of calcium do the same in mutant terminals.

Syt1, Syt2, and SV2B regulated expression during postnatal development

As motor dysfunction in SMA mice is present on the first day of postnatal life (42), we wondered whether the protein expression modifications observed in SMA terminals at P9-11 already existed earlier and whether they could be ascribable to the maturation delay previously described at the NMJ (4,6,43,44). Given that pre- and postsynaptic maturation normally evolves in parallel, we compared the structural features of WT and SMA NMJs at P3 and P9-11 in the TVA, in terms of endplate size (increases with age), shape (from full to perforated plate), and clustering of ACh receptors (evolving from spots to folders) (45,46). We found that the mean endplate surface area was not different in WT and mutant at P3, but reduced in mutants at P9-11 (Fig. 6A, left panel). We also quantified the number of endplates with ACh receptors clustered in spots (immature), folders (mature), and intermediate structures, as well as the number of endplates without perforations (immature), and with small, medium, and large perforations (mature). The results show that endplates of both genotypes maturate, although, mutants were already slightly lagged at P3 compared with WTs (Fig. 6A, right graphs).

Next, we explored the level of coexpression of Syt2 and Syt1 in individual synapses. At P3, all WT terminals expressed Syt1 and Syt2 (Fig. 6B, open symbols), contrarily to what was found at P9-11 where 71% of nerve terminals (27 out of 38) showed no Syt1 signal while the remaining 29% only displayed a small amount (Syt1/postsynaptic area ratio ≤ 0.06). These results indicate that a switch in the Syt-isoform during the postnatal maturation period occurs. In mutants, all terminals also expressed Syt1 at P3, but not all expressed Syt2 (Fig. 6B, dark symbols). The mean changes in Syt1 and Syt2 are represented in Part C of the figure. Notably, in both genotypes Syt1 and Syt2 levels changed oppositely with age, with Syt1 being downregulated, and Syt2 upregulated. The sum of both signals is also shown, as well as the change in SV2B levels (right graphs). Conversely to Syt levels, SV2B decreased in mutant terminals while it changed little during this time interval in WT terminals. Altogether, these data indicate that Syt1, Syt2, and SV2B expressions were decreased significantly from as early as P3 in mutants compared with WTs, at an age at which pre- and postsynaptic postnatal maturation changes were still very mild.

Discussion

In this study, we investigated possible molecular mechanisms responsible for the reduction in neurotransmitter release at SMA neuromuscular synapses, as well as the basis for the selective vulnerability of motoneurons in SMA. We addressed these two questions by the investigation of the changes in the expression of synaptic proteins in nerve terminals from muscles affected differently in the SMA mouse model together with a comprehensive functional analysis of the neurotransmission impairment. The two most relevant findings in the current study are: i) a large reduction of Syt2 and SV2B in SMA nerve terminals of all four studied muscles, together with an impairment in modulating the RRP size, and ii) the presence of different physiological presynaptic levels of Syt1 in nerve terminals from distinct muscles; high vulnerable muscles having much lower levels than less affected ones, in agreement with preliminary data in SMA type I human patients showing overexpression of this protein in resistant motoneuron pools (47).

What are the functional consequences of the low levels of Syt and SV2 isoforms in SMA synapses? Besides their function

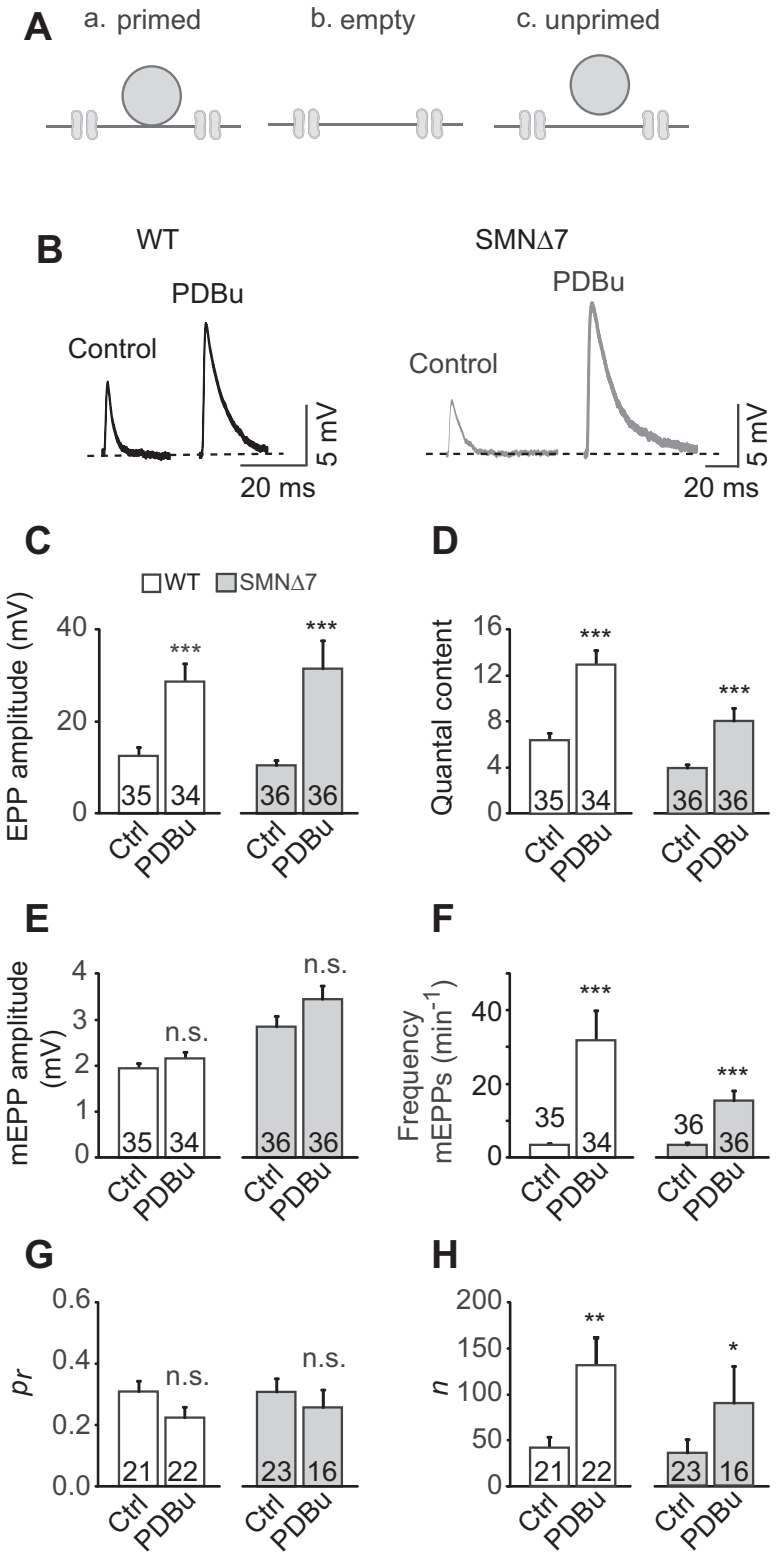

Figure 5. Phorbol 1,3 dybutirate (PDBu) increases synaptic responses in SMA motor nerve terminals. (**A**) Hypothetical states of the release site in WT and SMA terminals during stimulation. Calcium increase the number of functional release sites (left, primed vesicle), but not in mutants due to the scarcity of SVs (central, empty site), or to a defect in priming (right, unprimed vesicle). (**B-D**) Quantal release about doubled in WT and SMNΔ7 terminals in the presence of the Munc13/PKC activator PDBu (1 μM). (**E & F**) Mean mEPP amplitude was unchanged (E), but the frequency of spontaneous mEPPs was greatly increased by PDBu in both genotypes (F). (**G & H**) Release probability (p_r) was not changed, but the number of functional release sites was increased in both genotypes in the presence of the drug. All data are presented as mean ± SEM. U Mann-Whitney test. Numbers of fibres recorded inside bars. $n = 5$ mice per genotype. n.s.: not significant. *$P < 0.05$; **: <0.005; ***: $P \leq 0.0005$.

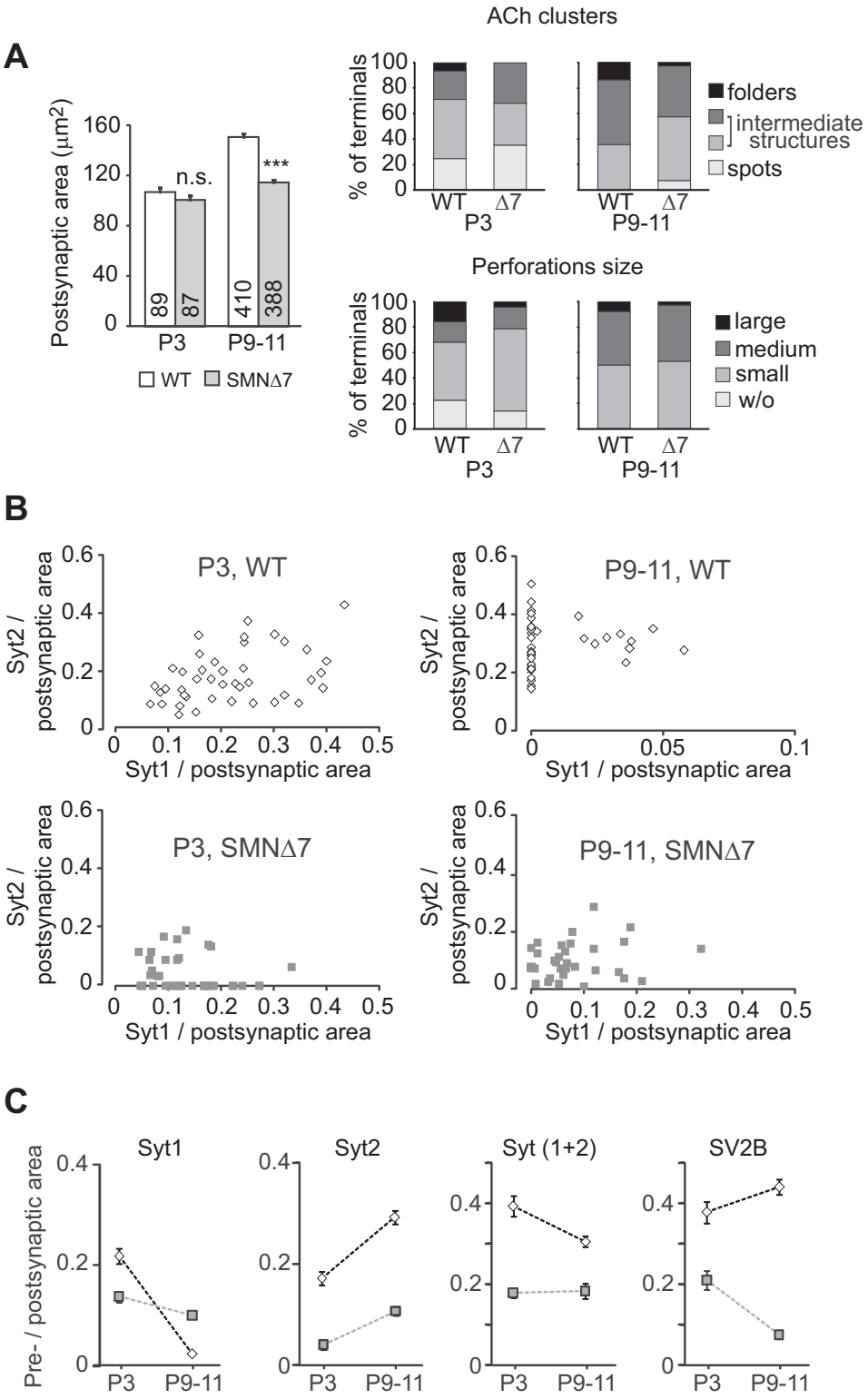

Figure 6. Early synaptic protein defects in motor nerve terminals of the TVA muscle in SMNΔ7 mice. (**A**) The postsynaptic size was not altered at P3 (left panel), but folders and perforations were slightly immature at P3 in mutants, as compared with P9-11 (right graphs). (**B**) Syt1 and Syt2 are co-expressed at P3, but not at P9-11 in all WT terminals, as determined by the immunostaining labelling of each protein in individual synapses. In mutant terminals, Syt1 and Syt2 were also co-expressed but at lower levels than in WT littermates (note the different X-axis scales). (**C**) As early as P3, Syt1, Syt2, and SV2B were significantly lower in SMA than in WT motor nerve terminals. Although physiological regulation of Syt2 and Syt1 occurred in WT and mutant terminals during postnatal maturation, the total amount of Syt-isoforms remained lower in mutants compared with WTs. SV2B greatly decreased with age only in mutants. Error bars indicate SEM. Numbers of terminals measured inside bars. $N \geq 3$ mice per genotype and protein isoform. Student *t*-test and Mann-Whitney *U* test. n.s.: not significant. ***: $P < 0.0005$.

as calcium sensors, Syt1 and Syt2 participate in vesicle docking (29), positional priming (32), and endocytosis (48,49). In fact, synchronous synaptic transmission is severely impaired in Syt1 and Syt2 knockouts (9,13,50), predicting that release would also be highly compromised in SMA neuromuscular synapses. On the other hand, the functional roles of SV2 isoforms are not completely established, but evidence indicates that they are key players in the regulation of the RRP size (31), priming (28,30), and presynaptic calcium concentration (20,28,51,52). In line with it, the synaptic alterations in SMA neuromuscular synapses (6–8) are comparable to the functional phenotypes of Syt2- or SV2-deficient mice (13,53). Additionally, electron microscopy studies have confirmed a reduction in the number of docked/primed vesicles at release sites in SMA motor nerve terminals from mice and humans (4,54). In accord with it, we found that the phorbol ester, PDBu, which increases priming independently of synaptotagmin action (55–57), enhanced neurotransmitter release in SMA by increasing the number of functional release sites (Fig. 5).

In addition to SV2 and Syt2, calcium channels (P/Q-type) were decreased in the TVA nerve terminals, comparable to the low expression of VDCCs (N-type) found in Smn-deficient motoneurons in culture (58). From a functional point of view, these results suggest that, on average, SVs in mutants experience a lower calcium concentration at release sites and could explain the significantly lower mean release probability of the nerve terminals in response to a single AP (Fig. 3C).

The origin of the synaptic changes at SMA NMJs is not clear yet. In SMA mice there is a maturation delay of the NMJ (4,6,43) what could affect the synaptic protein content and the release. The anomalous presence of Syt1 in SMA terminals at P10 (Fig. 1A and C) could be interpreted in this way. However, the following findings do not support that the maturation delay is the main cause of the synaptic alterations: i) not all synaptic proteins were altered (Fig. 2D) and, in those affected, the decrease was much beyond the differences in synaptic size ii) the switching of the calcium channel subtypes was not delayed (Fig. 4), iii) during postnatal development, SV2B decreased only in mutants (Fig. 6C), iv) the synaptic protein deficiencies were present at an early age (P3), a time at which the maturation defects seemed to be mild (Fig. 6), and v) in mild SMA mouse models, the maturation of the NMJ is normal, but secretion is impaired (59). Other possibilities for the synaptic defects are the dysregulation of the synthesis, transport, or stability of the altered synaptic proteins. SMN is linked to RNA metabolism (60,61), although, so far, no evidence exists that SMN controls synaptotagmin, P/Q-type VDCCs and/or SV2 transcripts. On the other hand, a selective defect in axonal transport affecting a particular molecular population of vesicles (62) cannot be discarded (63,64). Therefore, all these possibilities need to be further explored in future studies.

In conclusion, our findings shed light on the molecular mechanisms implicated in the neurotransmission dysfunction in SMA. Specifically, both the reduction in the number of calcium channels and the selective and substantial reduction of SV2B and Syt2, appear to underlie the impairment of stimulus-evoked neurotransmitter release observed in SMA motor nerve terminals in most affected muscles. We propose that the alteration in SV2B and Syt2 becomes critical in nerve terminals where Syt1 is physiologically downregulated, resulting in a greater vulnerability of the synapse. Also, our findings demonstrate the ability of phorbol ester to improve synaptic function in SMA terminals, which could be explored to complement current therapy approaches.

Materials and Methods

Animal model

Experimental mice were obtained by breeding pairs of SMNΔ7 carrier mice (*Smn+/-; SMN2+/+; SMNΔ7+/+*) on an FVB/N background (Jackson labs stain no. 005025). Identification of wild-type (WT) and SMA mice (*Smn-/-; SMN2; SMNΔ7*) was done by PCR genotyping of digital or tail DNA as previously described (42). Mice used in each experiment were either sex littermates at postnatal day 9 to 11 (P9-11), except in Figure 6 experiments that were done at P3 and P9-11. All experiments reported include the results of at least three animals per genotype, except for Syt7 that was two. All experiments were performed according to the guidelines of the European Council Directive for the Care of Laboratory Animals.

Muscle preparations

The *Transversus abdominis anterior* (TVA), the *Obliquus internus abdominis* (OIA), the rostral band of the *Levator auris longus* (LAL), and the diaphragm muscles were dissected with their nerve branches intact and pinned to the bottom of a 2.5 ml chamber, on a bed of cured silicone rubber (Sylgard, Dow Corning). Preparations were continuously perfused with a physiological solution of the following composition (in mM): 135 NaCl, 5 KCl, 1 $MgCl_2$, 12 $NaHCO_3$, 20 glucose, and 1 $CaCl_2$ (unless stated otherwise). The solution was continuously gassed with 95% O_2 and 5% CO_2, which maintained the pH at 7.35.

Ex vivo electrical stimulation and intracellular recording at the NMJ

Synaptic transmission recordings were performed *ex vivo* in acute neuromuscular preparations of the TVA muscle at room temperature. The nerve was stimulated using a suction electrode. The stimulation consisted of square-wave pulses of 0.2–0.5 ms duration and 2–40 V amplitude, at a frequency of 0.5 or 20 Hz. A glass microelectrode (10-30 MΩ) filled with 3 M KCl was connected to an intracellular recording amplifier (TEC-05X; npi electronic) and used to impale single muscle fibres near the motor nerve endings. Evoked endplate potentials (EPPs) and miniature EPPs (mEPPs) were recorded as described previously (34). The muscular contraction was prevented by including in the bath 3–5 μM μ-conotoxin GIIIB (Alomone Labs), a specific blocker of muscular voltage-gated sodium channels. The recording was performed at room temperature (22–23 °C).

Drugs

Studies of the expression of specific VDCCs in WT and SMA mice were performed in the presence of ω-agatoxin IVA (P/Q-type VDCC blocker) or ω-conotoxin GVIA (N-type VDCC blocker) (Alomone Labs), at a concentration of 200 nM and 1 μM, respectively. Phorbol (PDBu; Calbiochem) was dissolved in DMSO (Sigma-Aldrich) and used at 1 μM concentration.

Electrophysiological data analysis

The mean amplitudes of EPP and mEPPs recorded at each NMJ were normalized to -70 mV resting membrane potential. EPP amplitudes were corrected for nonlinear summation (65) as described previously (6). Quantal content (*m*) was estimated by the direct method. In the experiments with calcium blockers or

with low calcium concentration (≤0.75 mM), m was calculated by the indirect method (Ln (number of stimuli/number of failures)). To obtain actual values of p_r and n by binomial analysis (66,67) we measured EPP amplitudes during 100 shocks (at 0.5 or 20 Hz), calculated the mean m and the variance of m (Var(m)), and used the following equations: $p_r = (m - \text{Var}(m))/m$; $n = m/p_r$. All electrophysiological data are given as group mean values ± SEM unless otherwise stated.

Immunohistochemistry

Whole mount TVA, OIA, LAL, and diaphragm muscles from WT and SMA mice were fixed in 4% paraformaldehyde, washed in 0.1 M glycine in PBS for 30 min, permeabilized with 1% (v/v) Triton X-100 in PBS for 90 min, and incubated in 5% (w/v) BSA, 1% Triton X-100 in PBS for 3 h. Samples were incubated overnight at 4 °C with primary antibodies. Primary antibodies used were mouse monoclonal: Syt1 (1:250), or rabbit polyclonal: Syt2 (1:200), Syt7 (1:200), SV2A (1:500), SV2B (1:200), SV2C (1:200), P/Q-VDCC (1:500), Stx1B (1:1000), all from Synaptic Systems. Next day muscles were incubated for 1 h in PBS containing 0.05% Triton X-100, incubated for 1 h both with Alexa Fluor 647-conjugated goat anti-rabbit (Invitrogen), or CF488-conjugated donkey anti-mouse (Biotium), secondary antibodies and 10 ng/ml rhodamine-BTX and bathed again with 0.05% Triton X-100 for 90 min. Finally, muscles were mounted with slowfade medium (Invitrogen).

Imaging

Images were acquired with an upright Olympus FV1000 confocal microscope, equipped with three excitation laser lines (488, 561 and 633 nm). An alternating sequence of laser pulses was used during the acquisition of images for sequential activation of the different fluorescent probes. A 60x oil immersion objective (N.A. = 1.42) was used. Images from wild-type and littermate mutant preparations were taken with similar conditions (laser intensity and photomultiplier voltage) and, usually, during the same day. Only superficial nerve terminals were imaged. Fluorescence distribution and area were analysed using ImageJ routines. Presynaptic and endplate areas were delineated with outline masks based on brightness thresholding from maximal projected confocal images. In all IHC experiments, endplate ACh receptors were stained with BTX-Rho and the ratio between the fluorescent presynaptic area of interest and its BTX-Rho labelled endplate area was calculated for each NMJ (in figures, axis labelled as pre-/postsynaptic area). The background signal was subtracted using the same threshold used for the analysis of the presynaptic area.

Statistical analysis

Statistical analysis was performed with v.22 SPSS software. Statistical comparisons between SMA and WT measures or between one genotype in the absence versus presence of a drug were made using Student's t-test (two-tailed unless otherwise stated) when the distribution was normal, and U de Mann–Whitney rank sum test when the distribution was not normal. Normality was verified by the Kolmogorov-Smirnov test (for $n > 50$) or the Shapiro-Wilk test (for $n \leq 50$). Comparison of data from more than two groups was done by the ANOVA one factor test when the distribution was normal and by the Kruskal-Wallis test when the distribution was not normal. Results were considered statistically different when the P value was < 0.05. Significance was represented as follows: n.s.: not significant, *: $P < 0.05$, **: $P < 0.005$, ***: $P < 0.0005$. Each error bar represents SEM of the indicated number of experiments.

Acknowledgements

We are grateful to Bill Betz for useful discussions and comments on the manuscript.

Conflict of Interest statement. None declared.

Funding

This study was supported by the Spanish Ministry of Science and Innovation BFU2013-43763-P, BES2011-048901, BES-C-2014-0068 and by Fundación Tatiana Pérez de Guzman el Bueno. The authors declare no competing financial interests.

References

1. Lefebvre, S., Burglen, L., Reboullet, S., Clermont, O., Burlet, P., Viollet, L., Benichou, B., Cruaud, C., Millasseau, P., Zeviani, M., *et al.* (1995) Identification and characterization of a spinal muscular atrophy-determining gene. *Cell*, **80**, 155–165.
2. Burnett, B.G., Munoz, E., Tandon, A., Kwon, D.Y., Sumner, C.J. and Fischbeck, K.H. (2009) Regulation of SMN protein stability. *Mol. Cell. Biol.*, **29**, 1107–1115.
3. Fischer, U., Liu, Q. and Dreyfuss, G. (1997) The SMN-SIP1 complex has an essential role in spliceosomal snRNP biogenesis. *Cell*, **90**, 1023–1029.
4. Kong, L., Wang, X., Choe, D.W., Polley, M., Burnett, B.G., Bosch-Marce, M., Griffin, J.W., Rich, M.M. and Sumner, C.J. (2009) Impaired synaptic vesicle release and immaturity of neuromuscular junctions in spinal muscular atrophy mice. *J. Neurosci.*, **29**, 842–851.
5. Ling, K.K., Lin, M.Y., Zingg, B., Feng, Z. and Ko, C.P. (2010) Synaptic defects in the spinal and neuromuscular circuitry in a mouse model of spinal muscular atrophy. *PloS One*, **5**, e15457.
6. Ruiz, R., Casanas, J.J., Torres-Benito, L., Cano, R. and Tabares, L. (2010) Altered intracellular Ca2+ homeostasis in nerve terminals of severe spinal muscular atrophy mice. *J. Neurosci.*, **30**, 849–857.
7. Torres-Benito, L., Neher, M.F., Cano, R., Ruiz, R. and Tabares, L. (2011) SMN requirement for synaptic vesicle, active zone and microtubule postnatal organization in motor nerve terminals. *PloS One*, **6**, e26164.
8. Torres-Benito, L., Ruiz, R. and Tabares, L. (2012) Synaptic defects in SMA animal models. *Dev. Neurobiol.*, **72**, 126–133.
9. Geppert, M., Goda, Y., Hammer, R.E., Li, C., Rosahl, T.W., Stevens, C.F. and Sudhof, T.C. (1994) Synaptotagmin I: a major Ca2+ sensor for transmitter release at a central synapse. *Cell*, **79**, 717–727.
10. Maximov, A. and Sudhof, T.C. (2005) Autonomous function of synaptotagmin 1 in triggering synchronous release independent of asynchronous release. *Neuron*, **48**, 547–554.
11. Nishiki, T. and Augustine, G.J. (2004) Synaptotagmin I synchronizes transmitter release in mouse hippocampal neurons. *J. Neurosci.*, **24**, 6127–6132.
12. Angaut-Petit, D., Juzans, P., Molgo, J., Faille, L., Seagar, M.J., Takahashi, M. and Shoji-Kasai, Y. (1995) Mouse motor nerve terminal immunoreactivity to synaptotagmin II during sustained quantal transmitter release. *Brain Res.*, **681**, 213–217.

13. Pang, Z.P., Melicoff, E., Padgett, D., Liu, Y., Teich, A.F., Dickey, B.F., Lin, W., Adachi, R. and Sudhof, T.C. (2006) Synaptotagmin-2 is essential for survival and contributes to Ca2+ triggering of neurotransmitter release in central and neuromuscular synapses. *J. Neurosci.*, **26**, 13493–13504.
14. Boon, K.L., Xiao, S., McWhorter, M.L., Donn, T., Wolf-Saxon, E., Bohnsack, M.T., Moens, C.B. and Beattie, C.E. (2009) Zebrafish survival motor neuron mutants exhibit presynaptic neuromuscular junction defects. *Hum. Mol. Genet.*, **18**, 3615–3625.
15. Lazzell, D.R., Belizaire, R., Thakur, P., Sherry, D.M. and Janz, R. (2004) SV2B regulates synaptotagmin 1 by direct interaction. *J. Biol. Chem.*, **279**, 52124–52131.
16. Schivell, A.E., Batchelor, R.H. and Bajjalieh, S.M. (1996) Isoform-specific, calcium-regulated interaction of the synaptic vesicle proteins SV2 and synaptotagmin. *J. Biol. Chem.*, **271**, 27770–27775.
17. Yao, J., Nowack, A., Kensel-Hammes, P., Gardner, R.G. and Bajjalieh, S.M. (2010) Cotrafficking of SV2 and synaptotagmin at the synapse. *J. Neurosci.*, **30**, 5569–5578.
18. Bajjalieh, S.M., Frantz, G.D., Weimann, J.M., McConnell, S.K. and Scheller, R.H. (1994) Differential expression of synaptic vesicle protein 2 (SV2) isoforms. *J. Neurosci.*, **14**, 5223–5235.
19. Bajjalieh, S.M., Peterson, K., Shinghal, R. and Scheller, R.H. (1992) SV2, a brain synaptic vesicle protein homologous to bacterial transporters. *Science*, **257**, 1271–1273.
20. Janz, R. and Sudhof, T.C. (1999) SV2C is a synaptic vesicle protein with an unusually restricted localization: anatomy of a synaptic vesicle protein family. *Neuroscience*, **94**, 1279–1290.
21. Chakkalakal, J.V., Nishimune, H., Ruas, J.L., Spiegelman, B.M. and Sanes, J.R. (2010) Retrograde influence of muscle fibers on their innervation revealed by a novel marker for slow motoneurons. *Development*, **137**, 3489–3499.
22. Wu, Y.J., Tejero, R., Arancillo, M., Vardar, G., Korotkova, T., Kintscher, M., Schmitz, D., Ponomarenko, A., Tabares, L. and Rosenmund, C. (2015) Syntaxin 1B is important for mouse postnatal survival and proper synaptic function at the mouse neuromuscular junctions. *J. Neurophysiol.*, **114**, 2404–2417.
23. Bennett, M.R., Florin, T. and Hall, R. (1975) The effect of calcium ions on the binomial statistic parameters which control acetylcholine release at synapses in striated muscle. *J. Physiol.*, **247**, 429–446.
24. Miyamoto, M.D. (1975) Binomial analysis of quantal transmitter release at glycerol treated frog neuromuscular junctions. *J. Physiol.*, **250**, 121–142.
25. Searl, T.J. and Silinsky, E.M. (2003) Phorbol esters and adenosine affect the readily releasable neurotransmitter pool by different mechanisms at amphibian motor nerve endings. *J. Physiol.*, **553**, 445–456.
26. Wang, L.Y., Neher, E. and Taschenberger, H. (2008) Synaptic vesicles in mature calyx of Held synapses sense higher nanodomain calcium concentrations during action potential-evoked glutamate release. *J. Neurosci.*, **28**, 14450–14458.
27. Rosato Siri, M.D. and Uchitel, O.D. (1999) Calcium channels coupled to neurotransmitter release at neonatal rat neuromuscular junctions. *J. Physiol.*, **514 (Pt 2)**, 533–540.
28. Chang, W.P. and Sudhof, T.C. (2009) SV2 renders primed synaptic vesicles competent for Ca2+ -induced exocytosis. *J. Neurosci.*, **29**, 883–897.
29. Jorgensen, E.M., Hartwieg, E., Schuske, K., Nonet, M.L., Jin, Y. and Horvitz, H.R. (1995) Defective recycling of synaptic vesicles in synaptotagmin mutants of Caenorhabditis elegans. *Nature*, **378**, 196–199.
30. Nowack, A., Yao, J., Custer, K.L. and Bajjalieh, S.M. (2010) SV2 regulates neurotransmitter release via multiple mechanisms. *Am. J. Physiol. Cell Physiol.*, **299**, C960–C967.
31. Xu, T. and Bajjalieh, S.M. (2001) SV2 modulates the size of the readily releasable pool of secretory vesicles. *Nat. Cell Biol.*, **3**, 691–698.
32. Young, S.M., Jr. and Neher, E. (2009) Synaptotagmin has an essential function in synaptic vesicle positioning for synchronous release in addition to its role as a calcium sensor. *Neuron*, **63**, 482–496.
33. Haimann, C., Meldolesi, J. and Ceccarelli, B. (1987) The phorbol ester, 12-O-tetradecanoyl-phorbol-13-acetate, enhances the evoked quanta release of acetylcholine at the frog neuromuscular junction. *Pflugers Archiv: Eur. J.Physiol.*, **408**, 27–31.
34. Ruiz, R., Casanas, J.J., Sudhof, T.C. and Tabares, L. (2008) Cysteine string protein-alpha is essential for the high calcium sensitivity of exocytosis in a vertebrate synapse. *Eur. J.Neurosci.*, **27**, 3118–3131.
35. Malenka, R.C., Madison, D.V. and Nicoll, R.A. (1986) Potentiation of synaptic transmission in the hippocampus by phorbol esters. *Nature*, **321**, 175–177.
36. Nichols, R.A., Haycock, J.W., Wang, J.K. and Greengard, P. (1987) Phorbol ester enhancement of neurotransmitter release from rat brain synaptosomes. *J. Neurochem.*, **48**, 615–621.
37. Betz, A., Ashery, U., Rickmann, M., Augustin, I., Neher, E., Sudhof, T.C., Rettig, J. and Brose, N. (1998) Munc13-1 is a presynaptic phorbol ester receptor that enhances neurotransmitter release. *Neuron*, **21**, 123–136.
38. Gillis, K.D., Mossner, R. and Neher, E. (1996) Protein kinase C enhances exocytosis from chromaffin cells by increasing the size of the readily releasable pool of secretory granules. *Neuron*, **16**, 1209–1220.
39. Brose, N., Rosenmund, C. and Rettig, J. (2000) Regulation of transmitter release by Unc-13 and its homologues. *Curr.Opin. Neurobiol.*, **10**, 303–311.
40. Basu, J., Betz, A., Brose, N. and Rosenmund, C. (2007) Munc13-1 C1 domain activation lowers the energy barrier for synaptic vesicle fusion. *J. Neurosci.*, **27**, 1200–1210.
41. Schotten, S., Meijer, M., Walter, A.M., Huson, V., Mamer, L., Kalogreades, L., ter Veer, M., Ruiter, M., Brose, N., Rosenmund, C., *et al.* (2015) Additive effects on the energy barrier for synaptic vesicle fusion cause supralinear effects on the vesicle fusion rate. *eLife*, **4**, e05531.
42. Le, T.T., Pham, L.T., Butchbach, M.E., Zhang, H.L., Monani, U.R., Coovert, D.D., Gavrilina, T.O., Xing, L., Bassell, G.J. and Burghes, A.H. (2005) SMNDelta7, the major product of the centromeric survival motor neuron (SMN2) gene, extends survival in mice with spinal muscular atrophy and associates with full-length SMN. *Hum. Mol. Genet.*, **14**, 845–857.
43. Kariya, S., Park, G.H., Maeno-Hikichi, Y., Leykekhman, O., Lutz, C., Arkovitz, M.S., Landmesser, L.T. and Monani, U.R. (2008) Reduced SMN protein impairs maturation of the neuromuscular junctions in mouse models of spinal muscular atrophy. *Hum. Mol. Genet.*, **17**, 2552–2569.
44. Murray, L.M., Comley, L.H., Thomson, D., Parkinson, N., Talbot, K. and Gillingwater, T.H. (2008) Selective vulnerability of motor neurons and dissociation of pre- and post-synaptic pathology at the neuromuscular junction in mouse models of spinal muscular atrophy. *Hum. Mol. Genet.*, **17**, 949–962.

45. Sanes, J.R. and Lichtman, J.W. (2001) Induction, assembly, maturation and maintenance of a postsynaptic apparatus. *Nat. Rev. Neurosci.*, **2**, 791–805.
46. Sanes, J.R. and Lichtman, J.W. (1999) Development of the vertebrate neuromuscular junction. *Ann. Rev. Neurosci.*, **22**, 389–442.
47. Lee, J.C., Papandrea, D., Chung, W.K., Pisapia, D.J., Goldman, J.E. and Henderson, C.E. (2013) Identifying potential therapeutic targets in SMA through profiling of motor pools that show selective resistance in human patients and mouse models. *17th Annual International Spinal Muscular Atrophy Research Group Meeting*, **A30**.
48. Nicholson-Tomishima, K. and Ryan, T.A. (2004) Kinetic efficiency of endocytosis at mammalian CNS synapses requires synaptotagmin I. *Proc. Natl Acad. Sci. U S A*, **101**, 16648–16652.
49. Poskanzer, K.E., Marek, K.W., Sweeney, S.T. and Davis, G.W. (2003) Synaptotagmin I is necessary for compensatory synaptic vesicle endocytosis in vivo. *Nature*, **426**, 559–563.
50. Kochubey, O., Babai, N. and Schneggenburger, R. (2016) A Synaptotagmin Isoform Switch during the Development of an Identified CNS Synapse. *Neuron*, **90**, 984–999.
51. Custer, K.L., Austin, N.S., Sullivan, J.M. and Bajjalieh, S.M. (2006) Synaptic vesicle protein 2 enhances release probability at quiescent synapses. *J. Neurosci.*, **26**, 1303–1313.
52. Wan, Q.F., Zhou, Z.Y., Thakur, P., Vila, A., Sherry, D.M., Janz, R. and Heidelberger, R. (2010) SV2 acts via presynaptic calcium to regulate neurotransmitter release. *Neuron*, **66**, 884–895.
53. Janz, R., Goda, Y., Geppert, M., Missler, M. and Sudhof, T.C. (1999) SV2A and SV2B function as redundant Ca2+ regulators in neurotransmitter release. *Neuron*, **24**, 1003–1016.
54. Martinez-Hernandez, R., Bernal, S., Also-Rallo, E., Alias, L., Barcelo, M.J., Hereu, M., Esquerda, J.E. and Tizzano, E.F. (2013) Synaptic defects in type I spinal muscular atrophy in human development. *J. Pathol.*, **229**, 49–61.
55. Nagy, G., Kim, J.H., Pang, Z.P., Matti, U., Rettig, J., Sudhof, T.C. and Sorensen, J.B. (2006) Different effects on fast exocytosis induced by synaptotagmin 1 and 2 isoforms and abundance but not by phosphorylation. *J. Neuro.*, **26**, 632–643.
56. Rhee, J.S., Betz, A., Pyott, S., Reim, K., Varoqueaux, F., Augustin, I., Hesse, D., Sudhof, T.C., Takahashi, M., Rosenmund, C., *et al.* (2002) Beta phorbol ester- and diacylglycerol-induced augmentation of transmitter release is mediated by Munc13s and not by PKCs. *Cell*, **108**, 121–133.
57. Rosenmund, C., Sigler, A., Augustin, I., Reim, K., Brose, N. and Rhee, J.S. (2002) Differential control of vesicle priming and short-term plasticity by Munc13 isoforms. *Neuron*, **33**, 411–424.
58. Jablonka, S., Beck, M., Lechner, B.D., Mayer, C. and Sendtner, M. (2007) Defective Ca2+ channel clustering in axon terminals disturbs excitability in motoneurons in spinal muscular atrophy. *J. Cell Biol.*, **179**, 139–149.
59. Ruiz, R. and Tabares, L. (2014) Neurotransmitter release in motor nerve terminals of a mouse model of mild spinal muscular atrophy. *J. Anatomy*, **224**, 74–84.
60. Meister, G., Eggert, C. and Fischer, U. (2002) SMN-mediated assembly of RNPs: a complex story. *Trends in Cell Biol.*, **12**, 472–478.
61. Paushkin, S., Gubitz, A.K., Massenet, S. and Dreyfuss, G. (2002) The SMN complex, an assemblyosome of ribonucleoproteins. *Curr. Opin Cell Biol.*, **14**, 305–312.
62. Bonanomi, D., Benfenati, F. and Valtorta, F. (2006) Protein sorting in the synaptic vesicle life cycle. *Prog. Neurobiol.*, **80**, 177–217.
63. Dale, J.M., Shen, H., Barry, D.M., Garcia, V.B., Rose, F.F., Jr., Lorson, C.L. and Garcia, M.L. (2011) The spinal muscular atrophy mouse model, SMADelta7, displays altered axonal transport without global neurofilament alterations. *Acta Neuropathol.*, **122**, 331–341.
64. Jablonka, S., Wiese, S. and Sendtner, M. (2004) Axonal defects in mouse models of motoneuron disease. *J. Neurobiol.*, **58**, 272–286.
65. Martin, A.R. (1955) A further study of the statistical composition on the end-plate potential. *J. Physiol.*, **130**, 114–122.
66. Ruiz, R., Biea, I.A. and Tabares, L. (2014) alpha-Synuclein A30P decreases neurodegeneration and increases synaptic vesicle release probability in CSPalpha-null mice. *Neuropharmacology*, **76 Pt A**, 106–117.
67. Wang, X., Pinter, M.J. and Rich, M.M. (2010) Ca2+ dependence of the binomial parameters p and n at the mouse neuromuscular junction. *J. Neurophysiol.*, **103**, 659–666.